

**Semi-annual report for Grant NAG5-567 "Ionic Charge
Distributions of Energetic Particles from Solar Flares"**

D. J. Mullan

Bartol Research Foundation, University of Delaware, Newark, DE 19716

and

W. L. Waldron

Applied Research Corporation, Suite 650, 8401 Corporate Dr., Landover, MD
20785

This report covers the six-month period from July 1, 1985 to December 31, 1985.

The purpose of this research is to determine quantitatively the effects which solar flare X-rays have on the charge states of solar cosmic rays.

The charge states of the ions which are accelerated in association with solar flares have long been considered as of primary importance in providing us with fundamental physical information about conditions at the site of acceleration. The reason is obvious: the energetic particles may be "pure flare material", perhaps coming from the heart of the flare itself. If this is true, then we can sidestep the difficulties associated with interpreting other signatures of the flare, such as radiation in the visible, UV, X-ray, and radio portions of the spectrum. Those other signatures represent a complicated convolution of several factors, including local densities, optical depths, magnetic field strengths, energies of fast electrons and their spectra, etc. In contrast to these, detection of energetic particles allows us to "reach in" to the flare site and pluck out material which has experienced the flare phenomenon itself, and has now arrived at the detector, essentially unaffected by interplanetary effects, carrying "first-hand" information about the flare site.

The charge distributions of various ions contain information about the temperature at the acceleration site. If collisional processes were the only important determinant of the charge distributions, then a single parameter would characterize those distributions, namely, the local electron temperature. With this assumption, extensive tabular results have been compiled by several authors, showing the (unique) charge state distribution for each



N86-21487

Unclas
05685

CSCL 03B G3/92

(NASA-CR-176610) IONIC CHARGE DISTRIBUTIONS
OF ENERGETIC PARTICLES FROM SOLAR FLARES
Semiannual Report, 1 Jul. - 31 Dec. 1985
(Delaware Univ.) 10 p HC A02/NF A01

particular element. At any given temperature, each element can be characterized by a unique mean charge. Previous interpreters of the charge states of solar energetic particles (SEP) have generally adopted the approach of simply entering such tables with their observed mean charge value and reading off the appropriate temperature. We refer to this as an "ionization temperature", T_i .

Of course, if this were to be a physically meaningful temperature of the acceleration site, all of the elements whose charge states were recorded would yield identical values of T_i .

The problem is, the data definitely do *not* yield identical values of T_i . This problem has become especially acute with the extensive data compiled by ISEE-3. Thus, in a study of three large flares, Luhn et al (1984) reported $T_i = 2 \times 10^6 K$ for the elements C, N, O, Si, and S; $T_i = 4 \times 10^6 K$ for Ne and Fe; and $T_i = 7 \times 10^6 K$ for Mg. No stretching of the tables can possibly yield identical values of T_i for the three groups of elements. We therefore conclude that the straightforward interpretation of the observed charge states in terms of a "temperature" is not physically meaningful.

We proposed that the charge distribution would be seriously affected by X-rays from the flare. Hence, rather than characterizing the charge distribution by a single parameter ("temperature"), we proposed that a second parameter would be essential, namely, the X-ray flux at the acceleration site. We proposed to calculate quantitatively how the charge distributions would be altered in the presence of realistic flare X-ray spectra.

To model the effects of flare X-rays, we proceed as follows. The temperature structure of the solar atmosphere is taken to be basically two plateaus, one chromospheric (at $T = 9500 K$), the other coronal (at $T = 2 \times 10^6 K$). Between these two plateaus, there is a transition region where the temperature varies linearly with height over 25 km. In the absence of X-rays, the ionization structure can be calculated uniquely for each element in the corona. The flare is modelled as a source of X-rays located in the transition region, at a height of 5 km below the base of the corona. The temperature of the flare X-ray source is taken, in the first instance, to be $10^7 K$: this is entirely consistent with the measured X-ray spectra of many solar flares.

To model the effects of flares of varying size, we vary the emission measure of the X-ray source. Here, we are interested in one-dimensional X-ray penetration through the solar atmosphere. Thus, the emission parameter which we use here is a linear one, defined as

$$EML = N_e^2 \times \delta x$$

where N_e is the local electron density, and δx is a linear thickness of the X-ray emitting region. The values which we have explored for

\log_{10} EML so far range from 31.5 to 35.5 in steps of 0.25. For comparison, we note that the volumetric emission measures, EMV, of many solar flares lie in the range \log_{10} EMV = 48-50. Hence if the area of flare emission is of order \log_{10} area = $10^{15.5} \text{cm}^2$, our choice of linear emission measure is reasonable. Small solar flares have dimensions of order 10^8 cm, and thus it appears that our choice of areal factor is also empirically plausible. With a uniformly filled flare volume of side length 10^8 cm, our choice of EML values corresponds to electron densities in the range $\log_{10} N_e = 11.75-13.75$.

For purposes of calculating the charge distributions, we need to know the flux of X-rays which pass through unit area of a volume element in the solar corona near the flare. For this purpose, we have chosen to consider, in the first instance, a "target point" situated in the corona at a distance of 1000 km from the X-ray source. The latter is treated as a point, although clearly, it is trivial to allow for the finite extent of the source, and to move the "target point" to an arbitrary location. This choice of distance leads to X-ray fluxes at the "target point" which lie in the range from 5×10^7 to $5 \times 10^{11} \text{ergs cm}^{-2} \text{sec}^{-1}$.

In the equation of ionization balance, the ionization rate due to photons is proportional to the first power of the density, whereas the ionization rate due to collisions, and the recombination rate, are both proportional to the square of the density. Thus, in a steady state, where photoionizations are balanced by collisional recombinations, the charge state will depend on the ratio of X-ray flux to the local density. It is in terms of that ratio that we will characterize our results.

However, for definiteness in the calculations, we choose a coronal density of 10^{12}cm^{-3} . Hence, for the most part, the flare plasma which we have chosen to model is denser than the ambient corona, as we would expect.

The calculation proceeds as follows. The X-rays, with a thermal bremsstrahlung spectrum, are allowed to propagate through the ambient corona, ionizing the local material as they pass through. After propagating 1000 km, the local charge distributions are printed out for each of eight elements: H, He, C, N, O, Ne, Mg, Si, and S. For the first four of these elements, the quiet coronal conditions are already such that each of them is essentially stripped of its electrons. Thus, the dominant stages of ionization are H II, He III, C VII, and N VIII, even without X-rays. Addition of flare X-rays does not alter the ionization distribution in any qualitative way. For oxygen, O VII and O VIII are present in almost equal abundances in the ambient corona: adding flare X-rays pushes the dominant ionization stage higher, until O IX becomes dominant for $\log_{10} \text{EML} = 33.75$ and greater.

For the remaining four elements, we show in Figures 1-4 how the relative abundance of the various charge states alters as the X-ray flux builds up. For example, in the ambient corona, Ne is predominantly Ne IX, but with increasing X-ray flux, the predominant stage becomes Ne X and finally Ne XI (i.e. fully stripped), within the range of X-ray fluxes which we have considered. Suppose we tried to interpret the observation of completely stripped Ne in terms of collisional processes alone: then according to the tables of C. Jordan (1968), the "ionization temperature" would have to be at least as high as $5 \times 10^8 K$. However, as Fig. 1 shows, we can make Ne XI the dominant stage of ionization even when the ambient temperature is only $2 \times 10^6 K$ as long as the X-ray flux is large enough (but still reasonable as far as solar flares are concerned).

In Fig. 2, we show the results for magnesium. Here, within the range of X-ray fluxes which we have considered, we can drive magnesium to such a state that the predominant ion becomes the fully stripped one, Mg XIII. For this to occur by purely collisional processes, Jordan's tables suggest that the temperature would have to be at least $10 \times 10^6 K$: and yet, our ambient medium is still at only $2 \times 10^6 K$. Thus, the interpretation of a charge state of Mg in such conditions in terms of purely collisional processes would yield a source temperature which would be in error by 500%.

In Figs. 3 and 4, we show the ionization states for silicon and sulfur. Here, the presence of many competing levels of ionization makes for peculiar charge state distributions: the dominant charge state remains essentially unchanged in Si, for example, over a very broad range of X-ray fluxes. For sulfur, the situation is also complicated: the dominant charge state remains 9+ or 10+ over a broad range of X-ray fluxes, and then changes abruptly to 14+.

In Fig. 5 we show the "apparent ionization temperature" for four elements as a function of X-ray flux. The ordinate represents the temperature which the ambient medium would need to have in order to create the same predominant stage of ionization if the X-rays were entirely absent. (Note that H, He, C, N, and O would all lie on a horizontal line at a temperature of 2×10^6 in Fig. 5.) In general, we can characterize the results by the statement that Mg is the most sensitive element to the X-ray flux, Ne is next, and S/Si (along with H, He, C, N, and O) are the least sensitive.

In view of the empirical results of Luhn et al (1984), the results in Fig. 5 are of great interest. Qualitatively, the results of Luhn et al are in complete agreement with Fig. 5: the lowest "apparent ionization temperatures" are ascribed by Luhn et al to S, Si, C, N, and O, the highest are ascribed by them to Mg, with Ne lying in between. This is consistent with the right-hand side of Fig. 5.

Quantitatively, to reproduce the figure of $7 \times 10^6 K$ quoted by Luhn et al for Mg, we would need to have an X-ray flux to electron

density ratio of order -0.5 (in the logarithm to base 10). To reproduce the figure of $4 \times 10^6 K$ quoted by Luhn et al for Ne, we would need an X-ray flux to density ratio of order -1.0. And to reproduce the figure of $2 \times 10^8 K$ quoted by Luhn et al for Si and S, we would need an X-ray flux to density ratio of -1.5 or less. Thus, we cannot claim that we yet have obtained quantitative agreement to better than an order of magnitude with the results of Luhn et al. However, we note that we have made no attempt yet to optimize the quantitative agreement between our calculations and the results of Luhn et al: the results in Figs. 1-5 are a first cut through the problem, with values of solar coronal parameters which seemed plausible.

The fact that our first cut has yielded qualitative agreement with the empirical results is encouraging. We now plan to do a more detailed study of parameter space in order to discover whether or not we can improve on our quantitative accuracy. In particular, rather than depending solely on the mean charge state (as Luhn et al prefer to do), we plan to calculate the actual charge distribution to compare with the ISEE-3 data.

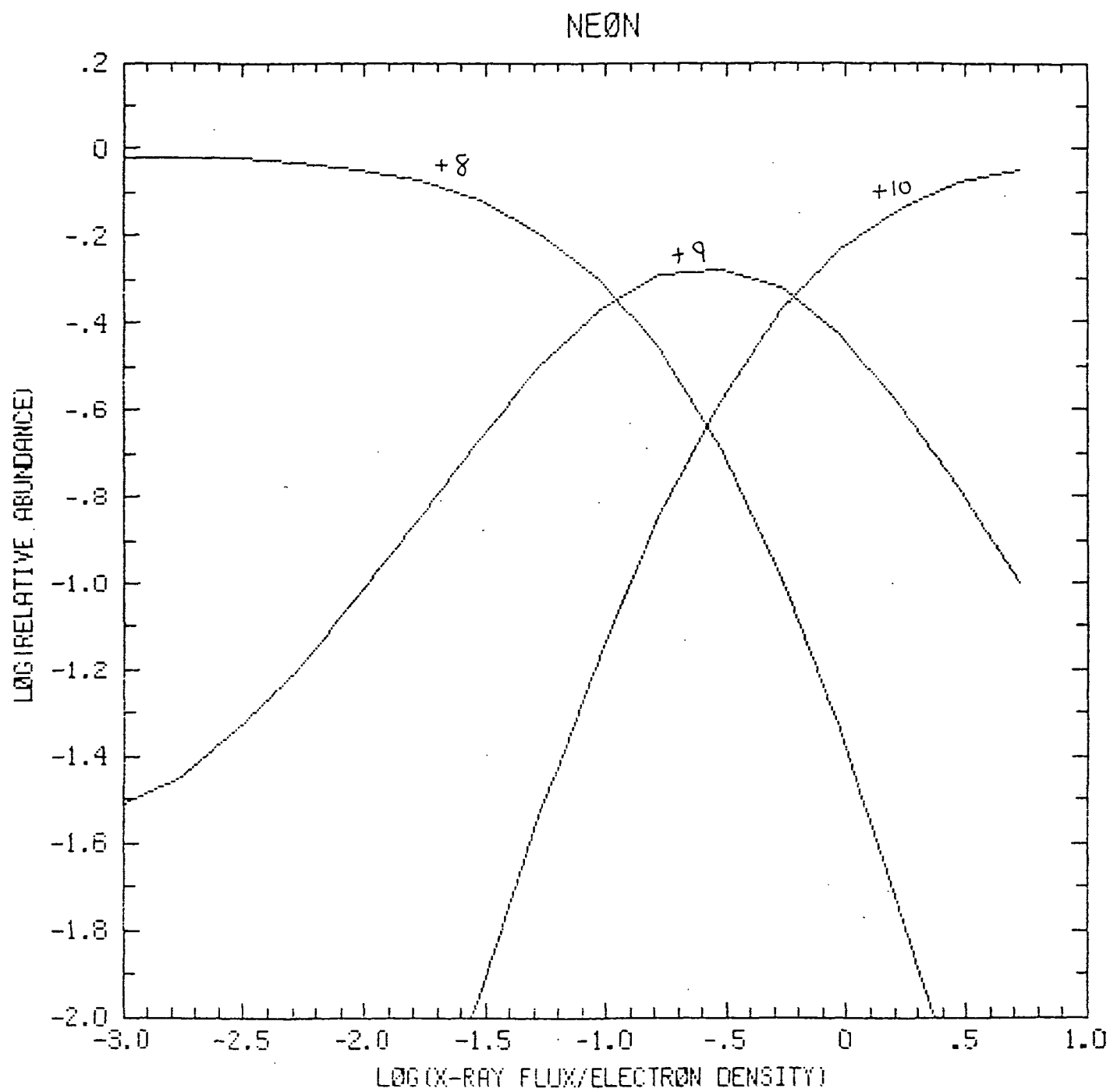


Fig. 1

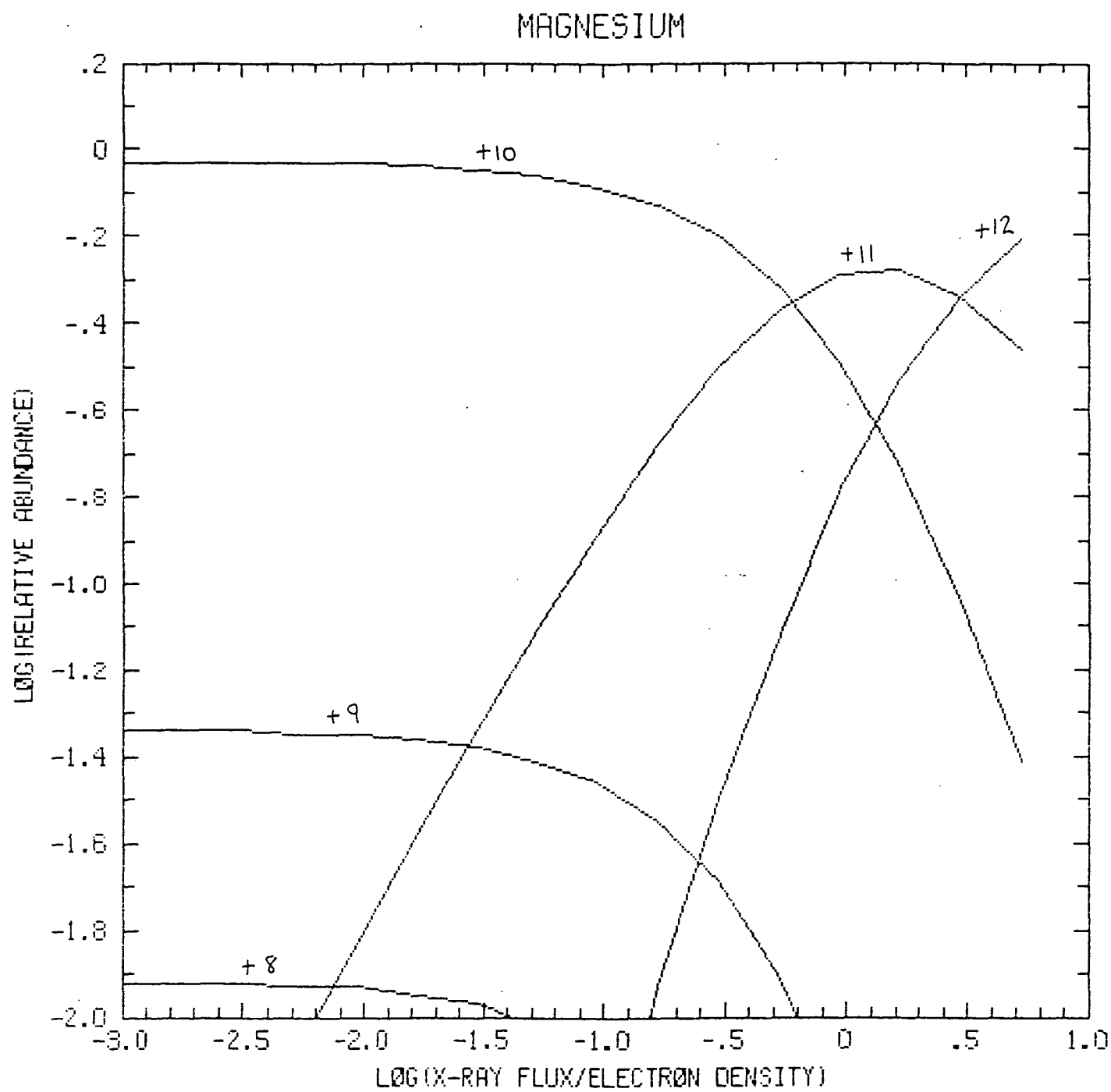


Fig. 2

SILICON

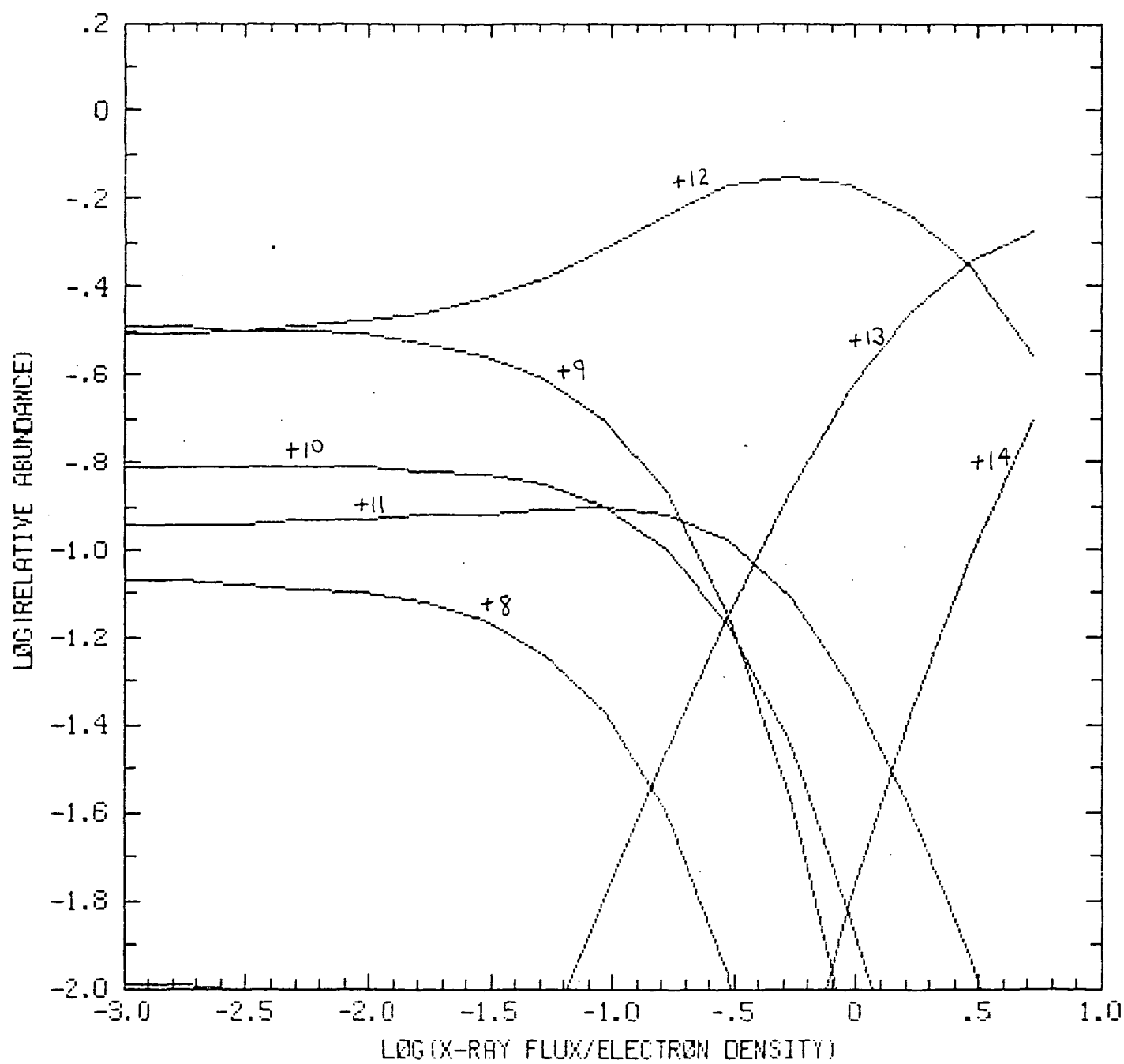


Fig. 3

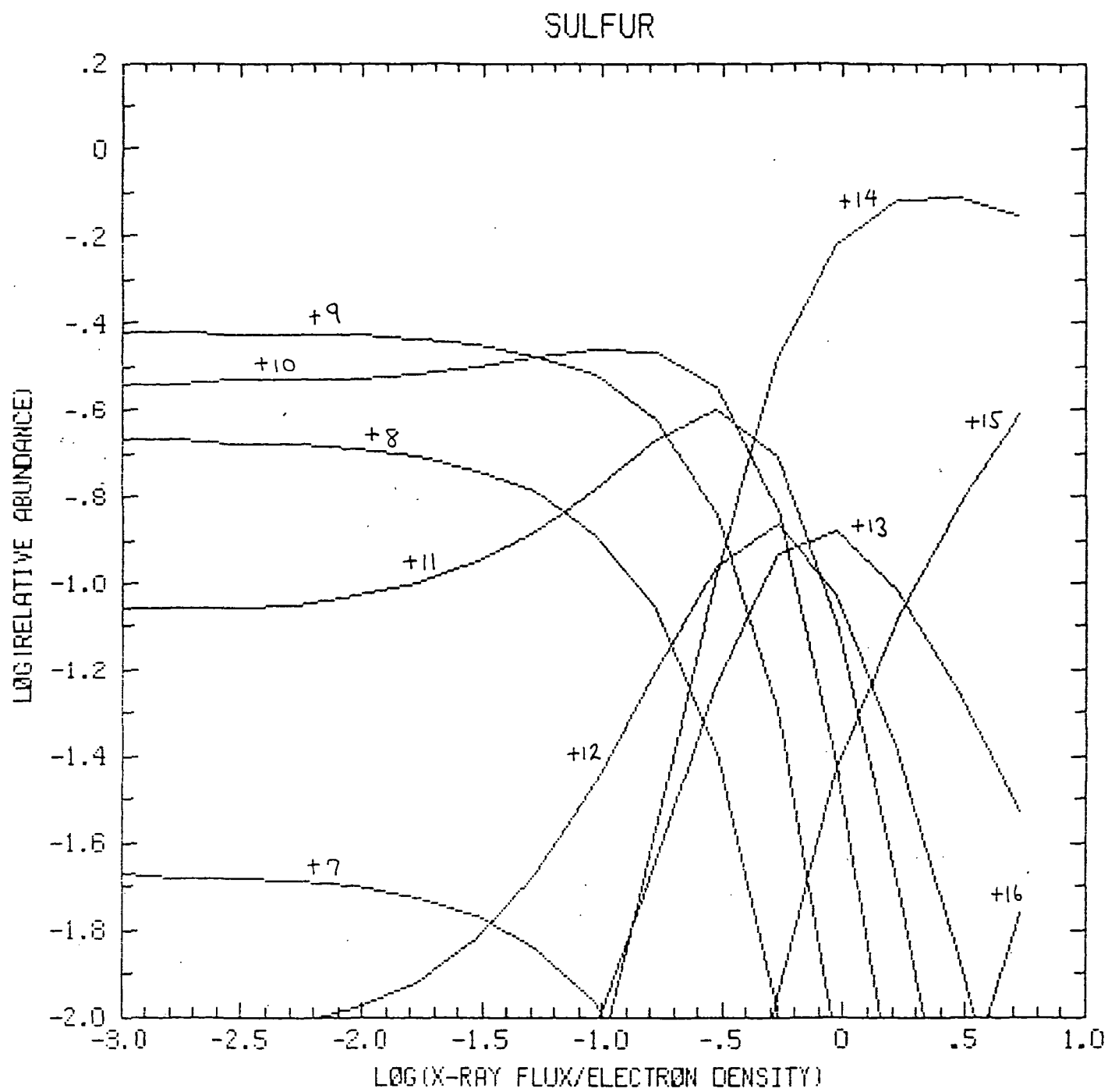


Fig. 4

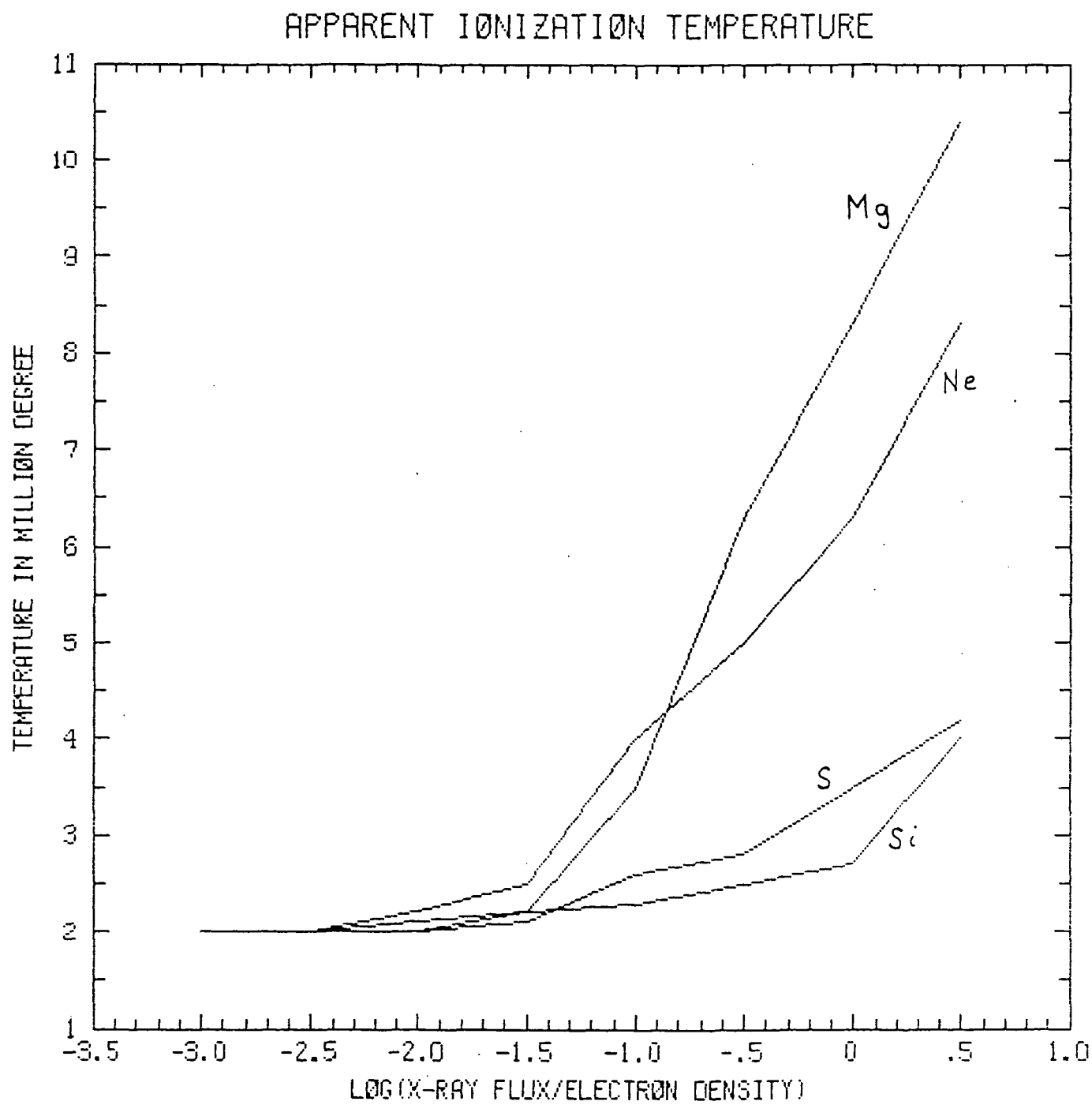


Fig. 5